



This is a repository copy of *Hypoxia modulates CCR7 expression in head and neck cancers*.

White Rose Research Online URL for this paper:
<http://eprints.whiterose.ac.uk/129656/>

Version: Accepted Version

Article:

Basheer, H.A., Pakanavicius, E., Cooper, P.A. et al. (5 more authors) (2018) Hypoxia modulates CCR7 expression in head and neck cancers. *Oral Oncology*, 80. pp. 64-73. ISSN 1368-8375

<https://doi.org/10.1016/j.oraloncology.2018.03.014>

Reuse

This article is distributed under the terms of the Creative Commons Attribution-NonCommercial-NoDerivs (CC BY-NC-ND) licence. This licence only allows you to download this work and share it with others as long as you credit the authors, but you can't change the article in any way or use it commercially. More information and the full terms of the licence here: <https://creativecommons.org/licenses/>

Takedown

If you consider content in White Rose Research Online to be in breach of UK law, please notify us by emailing eprints@whiterose.ac.uk including the URL of the record and the reason for the withdrawal request.



eprints@whiterose.ac.uk
<https://eprints.whiterose.ac.uk/>

Hypoxia modulates CCR7 expression in head and neck cancers

Haneen A. Basheer,^{1,2} Edvinas Pakanavicius,³ Patricia A. Cooper,¹ Steven D. Shnyder,¹ Lisette Martin,⁴ Keith D. Hunter,⁴ Victoria Vinader,¹ Kamyar Afarinkia^{1*}

¹The Institute of Cancer Therapeutics, University of Bradford, Bradford, BD7 1DP, United Kingdom.

²Faculty of Pharmacy, Zarqa University, PO Box 132222, Zarqa 13132, Jordan.

³Division of Biosciences, University College London, London WC1E 6BT, United Kingdom.

⁴School of Clinical Dentistry, University of Sheffield, Sheffield, S10 2TA, United Kingdom.

Correspondence should be addressed to KA (k.afarinkia@bradford.ac.uk)

Highlights

- Under hypoxia, the expression of CCR7 is elevated in both *in vitro* and *in vivo* models.
- There is a correlation between HIF-1 α and CCR7 in all head and neck clinical stages.
- Hypoxia contributes to a metastatic phenotype in HNC by upregulating CCR7.

Abstract

Background: The chemokine receptor CCR7 is expressed on lymphocytes and dendritic cells and is responsible for trafficking of these cells in and out of secondary lymphoid organs. It has recently been shown that CCR7 expression is elevated in a number of cancers, including head and neck cancers, and that its expression correlates to lymph node (LN) metastasis. However, little is known about the factors that can induce CCR7 expression in head and neck cancers.

Method: We compared the protein expression and functional responses of CCR7 under normoxia and hypoxia in head and neck cancer cell lines OSC-19, FaDu, SCC-4, A-253 and Detroit-562 cultured as monolayers, spheroids, and grown *in vivo* as xenografts in balb/c mice. In addition, we analysed the correlation between hypoxia marker HIF-1 α and CCR7 expression in a tissue microarray comprising 80 clinical samples with various stages and grades of malignant tumour and normal tissue.

Results: Under hypoxia, the expression of CCR7 is elevated in both *in vitro* and *in vivo* models. Furthermore, in malignant tissue, a correlation is observed between hypoxia marker HIF-1 α and CCR7 across all clinical stages. This correlation is also strong in early histological grade of tumours.

Conclusion: Hypoxia plays a role in the regulation of the expression of CCR7 and it may contribute to the development of a metastatic phenotype in head and neck cancers through this axis.

Keywords: CCR7, head and neck cancer, hypoxia, HIF-1 α , tumour grade, tumour stage

Abbreviations: APES = 3-aminopropyltriethoxysilane; DAPI = 4',6-diamidino-2-phenylindole; HIF = hypoxia inducible factor; HNC = head and neck cancer; LDH-A = lactate dehydrogenase A; LN = lymph nodes; TMA = tissue microarrays.

Introduction

Tumours occurring in the anatomical regions of the head and neck are the sixth most common types of cancer worldwide, with over 500,000 new cases and over 350,000 deaths reported every year. [1] A particularly unwelcome hallmark of head and neck cancers is the high incidence of metastasis, particularly to regional lymph nodes. In fact, by the time of diagnosis, nearly half of head and neck cancers have already metastasised to neck lymph nodes and one in ten has metastasised to distant organs. [2]

It is now well established that the chemotactic signalling axis involving chemokines CCL19 and CCL21 acting on cell surface chemokine receptor CCR7 plays an important role in lymph node (LN) metastasis in a number of cancers. In normal physiology, CCR7 is expressed on lymphocytes and mature dendritic cells. The activation of CCR7 by CCL21 and CCL19 released from the secondary lymphoid organs enables these cells to migrate against the chemokine gradient in and out of the lymph nodes. It has been hypothesised that cancer cells adopt this chemotactic axis, through upregulating the expression of CCR7; thus enabling them to invade the lymphatic system. [3] So far, the significance of the CCL19/CCL21-CCR7 axis in LN metastasis has been shown in pancreatic, [4] colorectal, [5] gastric, [6] melanoma [7], breast [8-9] and in the head and neck cancers. [10-21] In particular, these studies have shown that CCR7 expression is elevated in a wide range of oral and oropharyngeal clinical tumour tissue; that the elevation in CCR7 expression is associated with a metastatic phenotype [13] and correlates with the potential for cervical LN metastasis in a number of oral cancers; [12-18] and that CCR7 expression is a negative prognostic factor in many different head and neck cancers. [19-21] Moreover, intracellular pathways which are stimulated as a result of the activation of CCR7 are being identified, [10, 22-26] and we are now beginning to gain an understanding of the mechanisms by which this axis contributes to the biology of the tumour cell.

However, whilst the role of CCR7 axis in the expansion of head and neck cancers is apparent, with the exception of tumour-associated inflammation, [10] relatively little known of the factors which promote the upregulation of CCR7 expression on tumour cells.

It is well established that as tumours grow, poor and irregular development of blood vessels leads to the emergence of regions within the tumour lacking in oxygen (hypoxia) and nutrients. Whilst the level of oxygenation in tumours can be quite varied, [27] more physiologically relevant, "severe" hypoxia in particular is known to have a wide ranging and

profound influence on the tumour microenvironment, and to promote malignancy and metastasis in cancers, [28-29] including head and neck cancers [30,31] through a diverse number of pathways. Interestingly, one of those pathways involves the upregulation of chemotactic receptors, for example CXCR4, [32-36] on tumour cells which in turn increase their metastatic potential.

In view of the recent evidence linking CCR7 expression with hypoxia in breast [35] and lung [36] cancers, we hypothesised that hypoxia may also be a factor in promoting CCR7 expression in head and neck cancers. Therefore in this study we investigated whether CCR7 expression correlates with the emergence of hypoxia in head and neck cancers.

Materials and Methods

Cells and cell culture

All cell lines, except OSC-19, were obtained from European Collection of Cell Cultures (ECACC) UK, American Type Culture Collection (ATCC) or National Cancer Institute (NCI) Developmental Therapeutics Programme. OSC-19 was obtained from Japanese Collection of Research Bioresources (JCRB).

Reagents and methods

Recombinant CCL19 (catalogue number 361-MI-025) and CCL21 (catalogue number 366-6C-025) were purchased from R&D Systems (Abingdon, UK). For flow cytometry, CCR7 Alexa Fluor[®] 488 conjugated anti-human CCR7 antibody (catalogue number 353205, Biolegend) (2:100 dilution) and the corresponding isotype matched control antibody (catalogue number 400233, Biolegend) (2:100 dilution) were used. In Immunohistochemistry, deparaffinised 5 µm-thick xenograft or tissue sections were incubated with CCR7 primary antibody (rabbit monoclonal IgG; Abcam, ab32527) (1:1000 dilution) for 1 h room temperature; whilst for HIF-1α (Anti-HIF-1α antibody, Abcam, catalogue number ab51608, 1:100 dilution) and Ki-67 (1:100 dilution) detection, the antibodies were incubated overnight at 4°C. A vectastain ABC kit with 3,3-diaminobenzidine (DAB) as chromogen was used to visualise the proteins. For cellular immunofluorescence, cells were permeabilised using 0.1% Triton X-100 before treatment with CCR7 and Ki-67 primary antibodies and were detected using fluorescent secondary antibody (Alexa Fluor[®] 546 Donkey Anti-Rabbit IgG, life technologies, catalogue number A10040) for 1 h in the dark. For pimonidazole detection, spheroids were treated with pimonidazole for 2 h prior to fixation in Bouin's Solution and paraffin embedding.

Hypoxyprobe™-1 Fitc conjugated antibody was added for 2 h at 37 °C. Cell nuclei were visualised using blue fluorescent dye DAPI. Scratch assays were performed in a 24 well plate with cells in media containing 2% serum. Images were captured at 0 h and an appropriate time to observe a significant difference between the two control experiments with and without added chemokine. These times were 24 h (SCC-4), 18 h (OSC-19), 24 h (FaDu), 42 h (DLD-1), 21 h (SW-480) and 14 h (PC-3) and migrated areas were measured using ImageJ software (NIH, USA). [37]

Xenografts

Balb/c immunodeficient nude female mice (Envigo, Loughborough, U.K.), aged between 6 and 12 weeks were used. Throughout the study, all mice were housed in air-conditioned rooms in facilities approved by the United Kingdom Home Office to meet all current regulations and standards. All procedures were carried out under a United Kingdom Home Office Project License (PPL 40/3670). 1×10^6 Tumour cells in 100 μ L of cell culture medium were injected into both abdominal flanks of the mouse, and tumour growth was then monitored using calliper measurements. Once tumours reached a volume of 150 mm³, mice were euthanised, and the tumours excised and fixed in 10% neutral buffered formalin for 24 h before being processed for paraffin embedding. 5 μ m-thick tissue sections were then collected on to 3-aminopropyltriethoxysilane (APES) coated glass slides and allowed to dry at 37°C overnight.

Tissue microarray

Head and neck tissue microarrays slides (consecutive slides from block HN803c) were purchased from Insight Biotechnology Limited (Wembley, UK). The microarrays were prepared by the US Biomax Inc. (<https://www.biomax.us/>) and information on tumour extent (T), regional lymph nodes (N) and distant metastasis (M) was provided, along with patient clinical characteristics (see **Supplementary Information S1**). Biomax collects human tissues are under HIPPA approved protocols with the donor providing informed consent.

Analysis

General: All data is presented as the mean \pm standard deviation of at least 3 independent experiments. Graph construction and statistical analysis was performed using GraphPad Prism 7.03. Differences among groups were assessed using the ANOVA test. Differences

between two groups were assessed using a *t* test. P values were calculated to determine statistical significance of the results. **P* < 0.05 and ***P* < 0.01 were deemed significant.

Evaluation of CCR7 and HIF-1 α staining in microarrays: H-score system [38] was used for the evaluation of the staining level of CCR7 and HIF-1 α . Briefly, tumour cells were scored according to a pre agreed staining level intensity (**Supplementary Information S2**), and the H-score was subsequently generated by adding the percentage of strongly stained cell (x3), the percentage of moderately stained cell (x2), and the percentage of weakly stained cell (x1), over a possible range of 0–300. The scores were independently obtained by two expert pathologists (KDH and LM) and the correlation between the two independent scores was above 0.9. For statistical analysis, the mean of the two values was calculated and used. Statistical analyses for clinical samples between H-scores of CCR7 and HIF-1 α for each clinical stage (1, 2, 3 and 4) and lymph node metastasis were performed using Pearson correlation test and the significance of the results is represented by P value. Statistical differences between the H-score for CCR7 or HIF-1 α expression between tumour and non-malignant cells were evaluated using Mann-Whitney U test. Association between high expression and clinical characteristics was evaluated using Fisher exact test. High expression levels were assigned for H-score \geq 150 as the mid-way between the highest (300) and lowest (0) H-scores. **P* < 0.05 and ***P* < 0.01 were deemed significant. Statistical tests on clinical samples were performed using Python 2.7 SciPy 0.19.

Results and Discussions

CCR7 is expressed in head and neck cancer cell lines and the receptor is functionally active

We first set out to determine the expression of CCR7 in various head and neck cancer cell lines cultured as monolayers using immunofluorescence. We chose OSC-19 (metastatic tongue), FaDu (pharynx), SCC-4 (tongue), A-253 (submaxillary salivary gland) and Detroit-562 (metastatic pharynx). For comparison, the expression of CCR7 in a number of other cancer cells lines was also assessed. In all five head and neck cancer cell lines, we detected the presence of CCR7. (**Figure 1A**) As the cells are permeabilised, antibody can access and react with both cytoplasmic and membranous CCR7. Indeed, we observed that in the head and neck cancer cell lines, expression of CCR7 was mostly membranous (except SCC-4), yet we observed cytoplasmic expression of CCR7 in both COLO205 and SW480 (not shown) colorectal cancer cell lines. (**Figure 1A**)

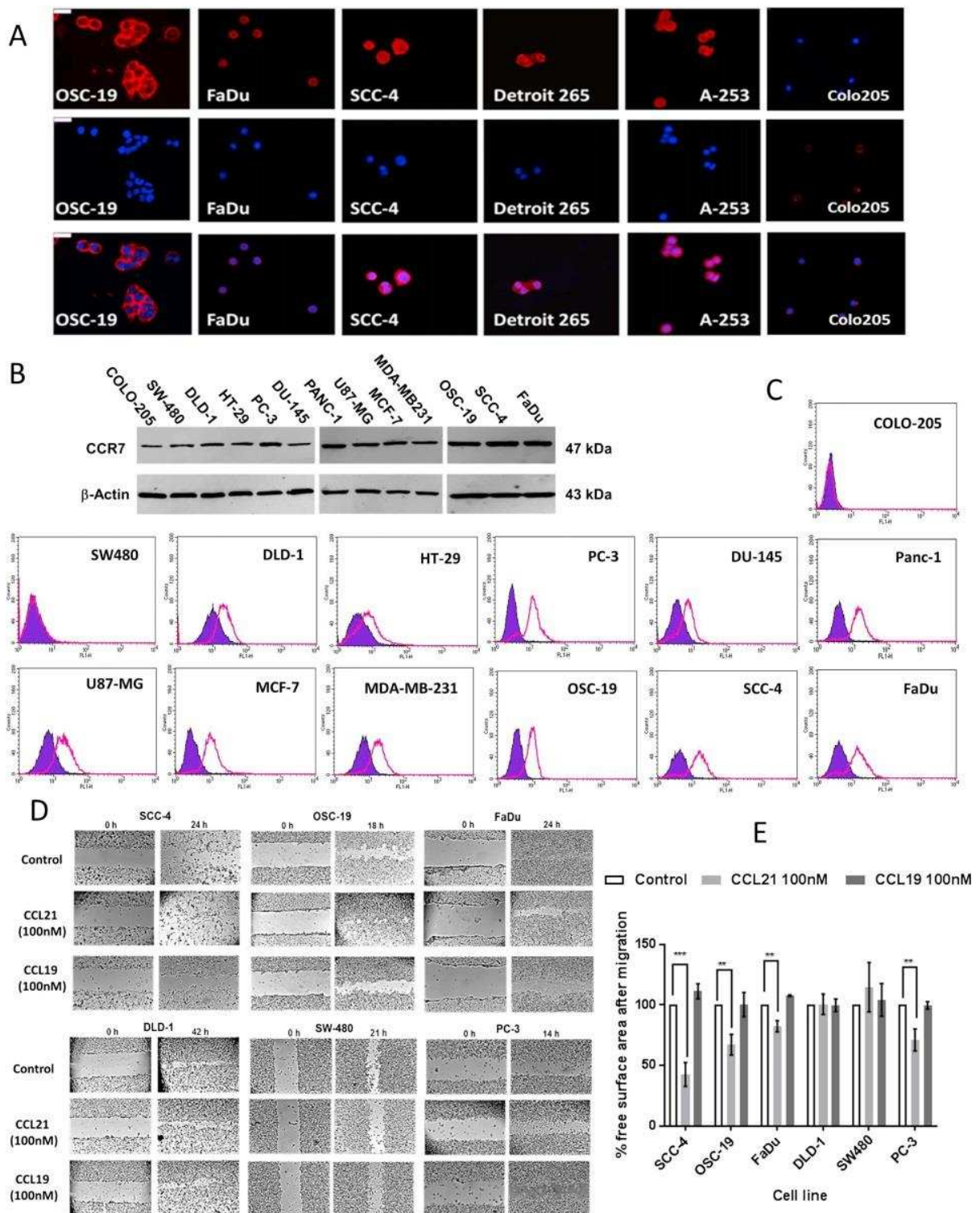


Figure 1: Expression and functional activity of CCR7 in cell lines: **(A)** Expression of CCR7 in head and neck cancer cell lines by immunofluorescence where blue represent staining for DAPI and red represent staining for CCR7. **(B)** Expression of CCR7 is detected in cancer cell lines by Western blot. **(C)** Expression of CCR7 in cancer cell lines by flow cytometry where the filled purple trace is the isotype control and cyan trace is the expression of CCR7. **(D)** Representative scratch assays. **(E)** Enhancement of cell motility in different cell lines upon treatment with CCL21 (100nM) and CCL19 (100nM) ($n = 3$). Two tailed T test P values are considered statistically different when ($P < 0.05$). SCC4 *** $p=0.0005$ (CCL21), $p=0.0647$ (CCL19); OSC19 ** $p=0.026$ (CCL21), $p=0.9686$ (CCL19); FADU ** $p=0.0031$ (CCL21), $p=0.076$ (CCL19); DLD1 $p=0.9234$ (CCL21), $p=0.9064$ (CCL19); SW480 $p=0.2838$ (CCL21), $p=0.6270$ (CCL19); PC3 ** $p=0.0052$ (CCL21), $p=0.7871$ (CCL19).

Using Western blot technique, CCR7 was ubiquitously detected in a wide range of cancer cell lines (**Figure 1B**). To quantify the levels of CCR7, we used flow cytometry and measured the expression of membranous protein using isotype antibody as control for non-specific binding (**Figure 1C**). There was general agreement between Western blot and flow cytometry results, although interestingly, not in all cell lines (e.g. SW480 and COLO205). A similar observation was previously reported by Na *et al.* [39] which showed that defects in the signal peptide domain of CCR7 can lead to the accumulation of cytoplasmic protein, which is unable to translocate to the cell membrane. Since Western blot analysis is carried out on whole cell lysates, it may have overestimated the relative presence of membranous CCR7 receptor in SCC-4 cell line.

In addition to demonstrating that the above head and neck cancer cell lines express CCR7, we also confirmed that the receptors are functionally active. In a scratch assay for OSC-19, FaDu and SCC-4, cell motility was increased in the presence of CCL21, a ligand for CCR7 (**Figure 1D**). Interestingly, the cell lines' response to CCL19 was less pronounced. This is consistent with reports from other laboratories that have shown CCL21 is better at inducing migration [40] and probably reflects the difference in the intracellular pathways activated by the two ligands. [41] In control experiments, the colon cell line DLD-1 and SW480 which express little CCR7, showed no increase in motility in the presence of CCL21 whilst CCR7 expressing prostate PC-3 cell line did (**Figure 1D, 1E**).

Whilst our results showed that head and neck cancer cell lines grown as monolayers express CCR7, we wanted to ensure that the CCR7 expression is maintained when the cells are grown as aggregates or as xenografts *in vivo*. There is evidence that cells can change their expression profiles when grown as multicellular spheroids or if xenoplated in mice. For instance, ovarian cancer cell lines are known to change the expression pattern of several proteins. [42] In head and neck cancers similarly, the significance of tumour microenvironment to factors that influence disease progression has also been highlighted. [43]

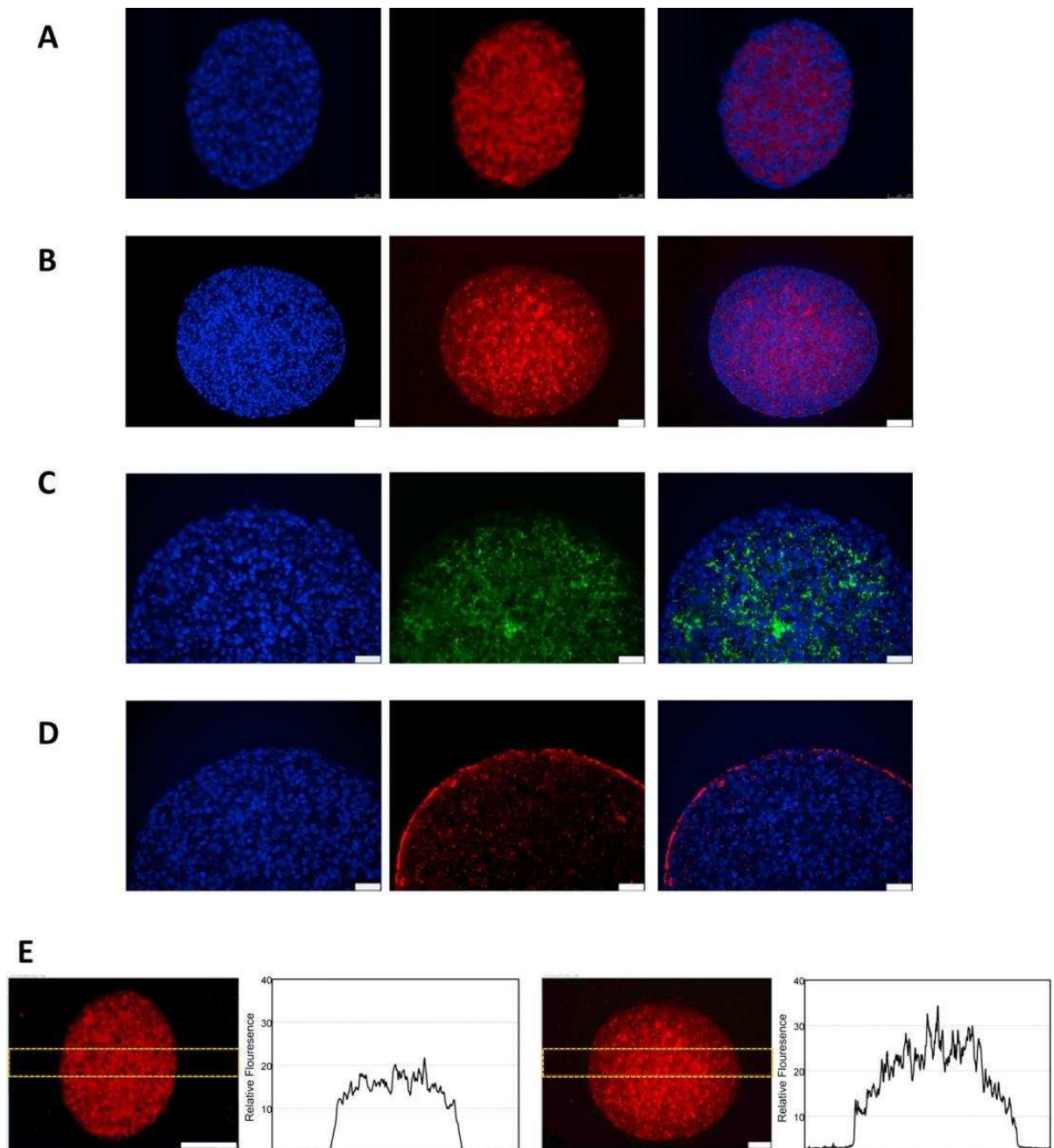


Figure 2: Expression and functional activity of CCR7 in multicellular spheroids: **(A)** Expression of CCR7 in a small spheroid where blue represents staining for DAPI and red represents staining for CCR7. Scale bar = 25 μm at 20x magnification **(B)** Expression of CCR7 in a larger spheroid shows more red staining in the core. Scale bar = 50 μm at 40x magnification **(C)** Presence of hypoxia in the core of larger spheroid is shown by immunofluorescence staining for pimonidazole adducts. **(D)** Proliferating rim of larger spheroid is shown by immunofluorescence staining for Ki-67. **(E)** Distribution of CCR7 as detected by immunofluorescence is uniform in smaller spheroid but elevated in the core of larger spheroid.

To determine the expression of CCR7 in *in vitro* 3D models, OSC-19 cells were grown as multicellular spheroids, formalin fixed and embedded in paraffin before sections were taken and analysed by immunofluorescence. The results (**Figure 2A**) clearly show that CCR7 expression is preserved in the cells within the spheroid. Furthermore, OSC-19, FaDu, A-253, and Detroit-562 cells were injected subcutaneously into mice and grown as tumours,

excised, formalin fixed and embedded in paraffin before sections were taken and analysed by immunohistochemistry. Again, we observed that mostly membranous CCR7 expression is preserved in the cells within the different xenoplated tumour tissues. The cytoplasmic expression of CCR7 was strongest in FaDu derived xenograft tissue. (**Figure 3**) Expression of CCR7 was also confirmed in clinical tissue (*vide infra*).

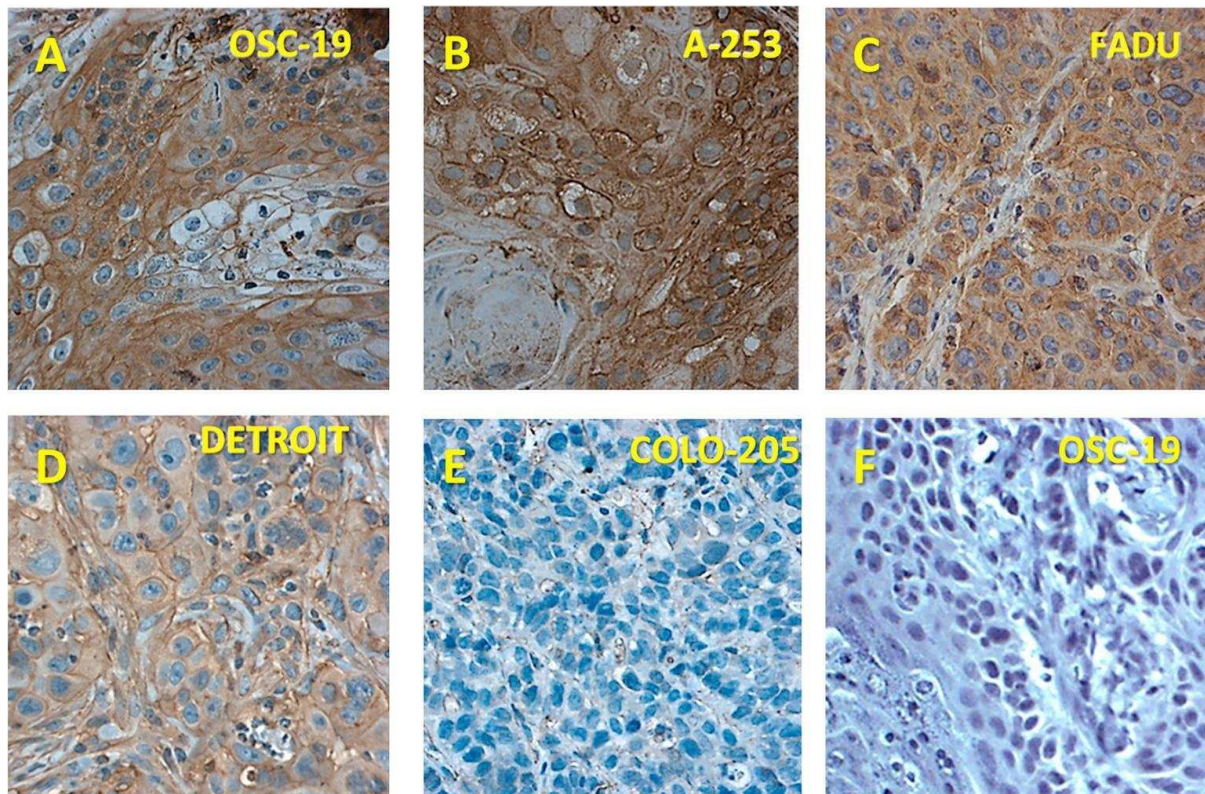


Figure 3. Expression of CCR7 in xenografts derived from different head and neck cells lines Protein expression (brown) is identified by biotinylated-labelled antibody. Basophilic structure of cell (blue) was counter stained with haematoxylin solution. **A**, OSC-19; **B**, A-253; **C**, FaDu; **D**, Detroit-256; **E**, COLO205. Negative control for OSC-19 is also shown, **F**. Scale bar = 100 μ m at 40x magnification

CCR7 protein expression increases under hypoxia in both *in vitro* and *in vivo* models

We next turned our attention to the role of hypoxia in CCR7 receptor expression. We quantitatively compared the cell surface expression of CCR7 in OSC-19 cells incubated under hypoxic and normoxic conditions. We found that all head and neck cancer cell lines, except SCC-4, increased their CCR7 expression under hypoxic conditions compared to cells incubated under normoxia. (**Figure 4A-B**) In particular, OSC-19 cells increased their CCR7 expression by 2.5 fold as measured by flow cytometry.

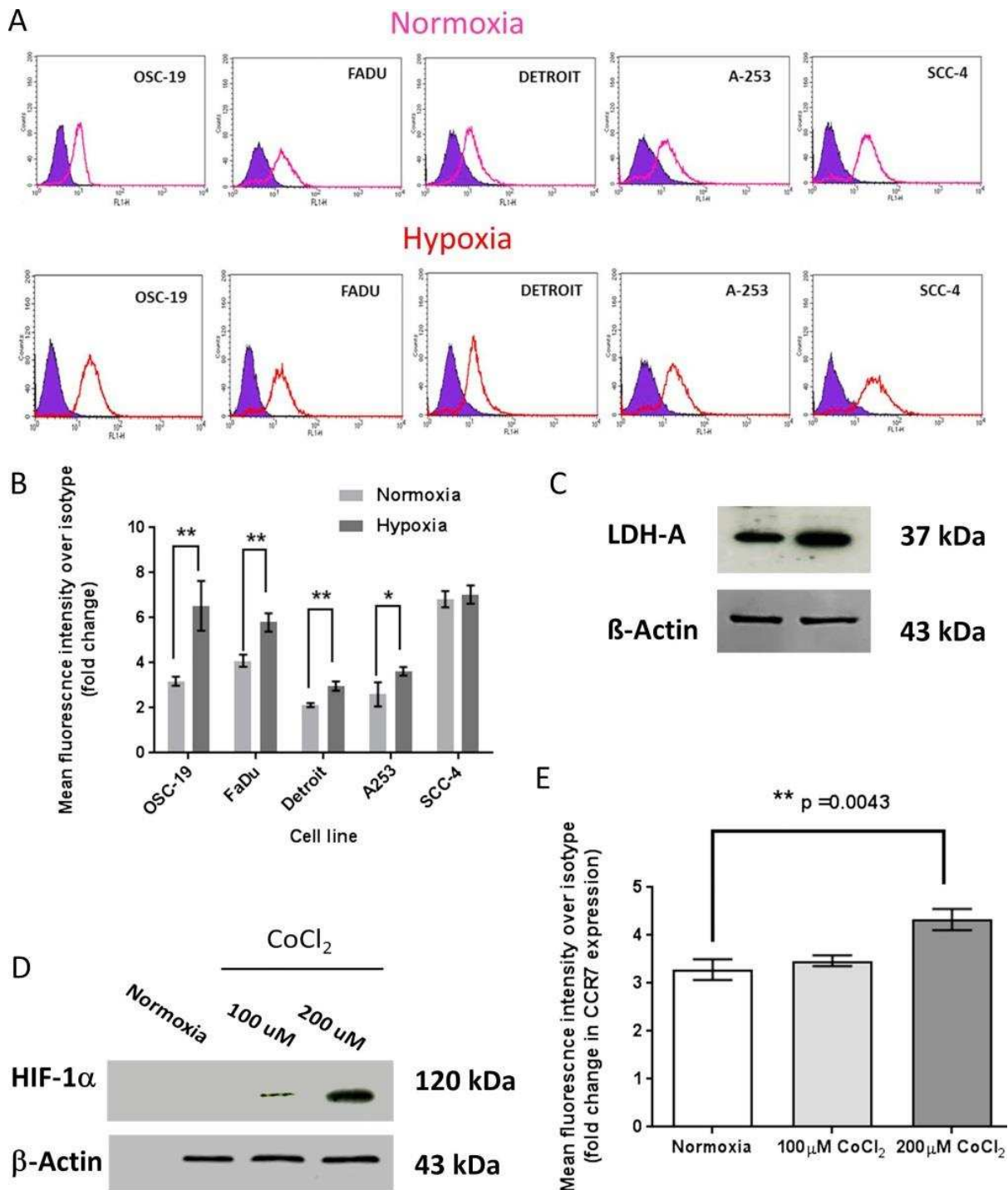


Figure 4. (A) Flow cytometry histograms showing relative expression of CCR7 under normoxia and under physiologic hypoxia (0.1% O₂) (B) bar chart showing relative expression of CCR7 in different head and neck cancer cell lines. All expression levels are normalised to isotype (n = 3). Two tailed T test P values are considered statistically different when (P < 0.05): OSC19 **p=0.0067; FADU **p=0.0038; Detroit **p=0.0032; A253 *p=0.0351; SCC4 p=0.5537. (C) Levels of lactate dehydrogenase-A (LDH-A), a downstream indicator of HIF-1 α mediated hypoxic response is elevated in OSC-19 cells under hypoxia. (D) Treatment of OSC-19 cells with CoCl₂ induces HIF-1 α . (E) Treatment of OSC-19 cells with CoCl₂ results in an increase in CCR-7 expression (n=3), 100 μ M CoCl₂ p=0.2574, **, 200 μ M CoCl₂ **p=0.0043.

A well-known feature of hypoxia in cells is the induction of transcription factors HIF-1 and HIF-2, with the former being the more commonly studied, as well as downstream proteins

such as lactate dehydrogenase A (LDH-A). [44,45] HIFs upregulate various cellular proteins in response to hypoxia, in order to compensate for the lack of available oxygen to the cell. [45,46] HIF-1 is comprised of two subunits: HIF-1 β , which is constitutively expressed and HIF-1 α , levels of which are suppressed by oxygen sensing proteins under normoxia. Under hypoxia, however, intracellular levels of HIF-1 α increase, which in complex with HIF-1 β leads to transcriptional changes in the cell. Although there are non-hypoxic mechanisms leading to the elevation of intracellular levels of HIF-1 α , [47,48] detection of elevated HIF-1 α or HIFs' downstream proteins such as LDH-A [44] is generally considered to be an indicator of hypoxia. Indeed, we showed that in OSC-19 cells, levels of LDH-A are elevated under hypoxia. **(Figure 4C)**

Stabilisation of HIF-1 α can also be achieved by addition of CoCl₂ to cell culture medium to mimic hypoxia. [49] So we next looked at the relationship between CCR7 and chemically induced (CoCl₂) hypoxia. Indeed, addition of CoCl₂ to OSC-19 cell culture medium, resulted in a dose dependent increase in HIF-1 α . **(Figure 4D)** A parallel increase in levels of CCR7 expression in the same cells was similarly detected by flow cytometry. **(Figure 4E)**

Of course, whilst exposure of cell monolayers to low oxygen conditions, or the use of CoCl₂ to mimic hypoxia are useful models, neither realistically recapitulates the conditions experienced by cancer cells in tissue. In this context, multicellular spheroids provide a convenient *in vitro* tool which can better emulate the conditions experienced by cancer cells which are within a matrix. For example, since gas perfusion through cell layers is restricted, an oxygen gradient is established towards the core of spheroids which mimics hypoxia in tumours. Generally speaking 200 μ m is considered the depth where oxygen levels fall to that seen in severe hypoxia (around 0.1% O₂), therefore spheroids with a radius greater than that are expected to have a hypoxic core. [50]

Indeed, analysis of the CCR7 expression in small and larger spheroids demonstrates that in the latter, the expression of the protein is higher in the hypoxic core compared to the oxygenated rim. When sections from a 230 μ m diameter OSC-19 spheroid, which was formalin-fixed and embedded in paraffin, were stained for CCR7 by immunofluorescence, we observed a uniform distribution of fluorescence intensity. However, when sections from a 500 μ m diameter OSC-19 spheroid were stained for CCR7 by immunofluorescence, the intensity of fluorescence in the core of the spheroids was relatively higher than in the periphery. **(Figure 2B, 2E)** To confirm the presence of hypoxia in the larger spheroid core,

the spheroids were treated with pimonidazole [51] prior to fixing and embedding in paraffin. Cellular proteins which react with pimonidazole were visualised by immunofluorescence which clearly showed more fluorescence in the spheroid core confirming existence of hypoxia. (**Figure 2C**) In addition, a marker of proliferation, Ki-67 [52] was more strongly detected as predicted in the non-hypoxic rim of the spheroid. (**Figure 2D**)

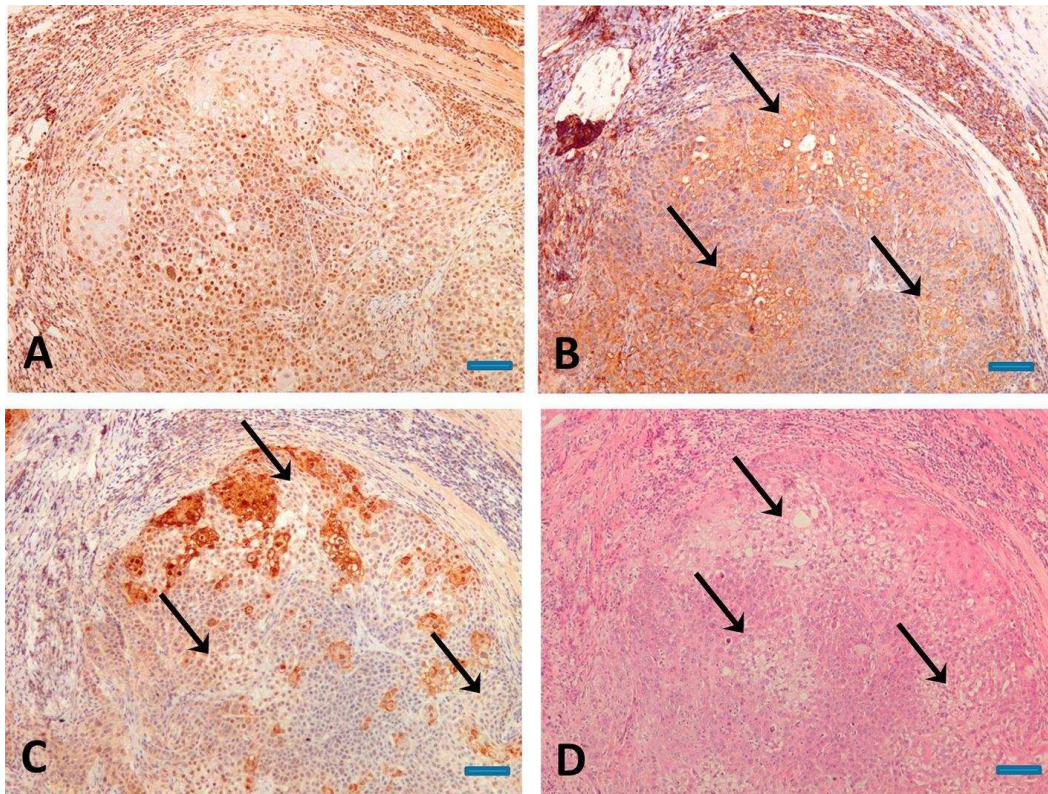


Figure 5. Staining of sequential sections from the A-253 xenografted tissues for Ki-67, (A); CCR7,(B); HIF-1 α , (C); and hematoxylin/eosin (H&E), (D). Scale bar = 100 μ m

Having shown a correlation between hypoxia and CCR7 expression in 2D and 3D *in vitro* models, we next turned our attention to *in vivo* models. We had previously shown (above) that head and neck cancer cell lines maintain expression of CCR7 when grown as xenografts in mice. Therefore, we set out to analyse the correlation between the expression of CCR7, and hypoxia in xenotransplanted tissue from head and neck cancer cell line A-253 as an example. (**Figure 5**) Sequential tissue sections were immunolabelled for CCR7, HIF-1 α as an indicator of hypoxia, Ki-67 as a marker for proliferating cells, as well staining with haematoxylin and eosin (H&E) to assess tumour morphology. (**Figure 5A**) Analysis of the tissue sections showed immunolocalisation of CCR7 across the tumour, but labelling intensity was higher in the vicinity of the hypoxic regions as indicated by HIF-1 α nuclear

localisation. (**Figure 5B and C**) The elevation of CCR7 in the hypoxic/necrotic region of the xenografted tumour was also confirmed with H&E staining. (**Figure 5B and D**)

Correlation between CCR7 protein expression with tumour grade and HIF-1 α in clinical tissue

Having shown a correlation between CCR7 and HIF-1 α *in vitro* and *in vivo*, we turned our attention to the analysis of the correlation between the two in clinical tissue. Consecutive slides from tissue microarrays (TMAs) with 80 patient cores (**Table 1** and **Supplementary Information S1**) were labelled with HIF-1 α and CCR7, and were scored independently for both using the H-score system, with the correlation (R) between the two independent scorers being >0.9. We first established that CCR7 expression is elevated in malignant tissues compared to non-malignant samples using the Mann-Whitney U test (P = 0.007). (**Figure 6A**) In contrast, we did not observe a correlation between malignancy and HIF-1 α expression. Interestingly, we found a correlation between higher expression of CCR7 (H-score > 150) with the clinical stage of cancer, and this is also strong in stage 1 compared to non-malignant tissues. (**Table 1**) In contrast, we found no correlation between higher expression of HIF-1 α (H-score > 150) and any clinical stages (**Table 1**). Similarly, we observed an association between expression of both CCR7 and HIF-1 α in histological grade 1 tumours compared with non-malignant tissue, with P = 0.0001 and 0.018 respectively for CCR7 and HIF-1 α . (**Table 2**)

	CCR7			HIF-1 α		
	Low (n)	High (n)	P	Low (n)	High (n)	P
non-malignant	9	2		9	2	
Stage 1	0	6	P=0.002**	2	4	P=0.1
Stage 2	12	11	P=0.14	18	5	P=1
Stage 3	8	11	P=0.06	17	2	P=0.6
Stage 4	5	8	P=0.05*	10	3	P=1
LN metastasis	3	5	P=0.07	6	2	P=1

Table 1: Association of high expression of CCR7 or HIF-1 α with head and neck cancer in different stages of the disease.

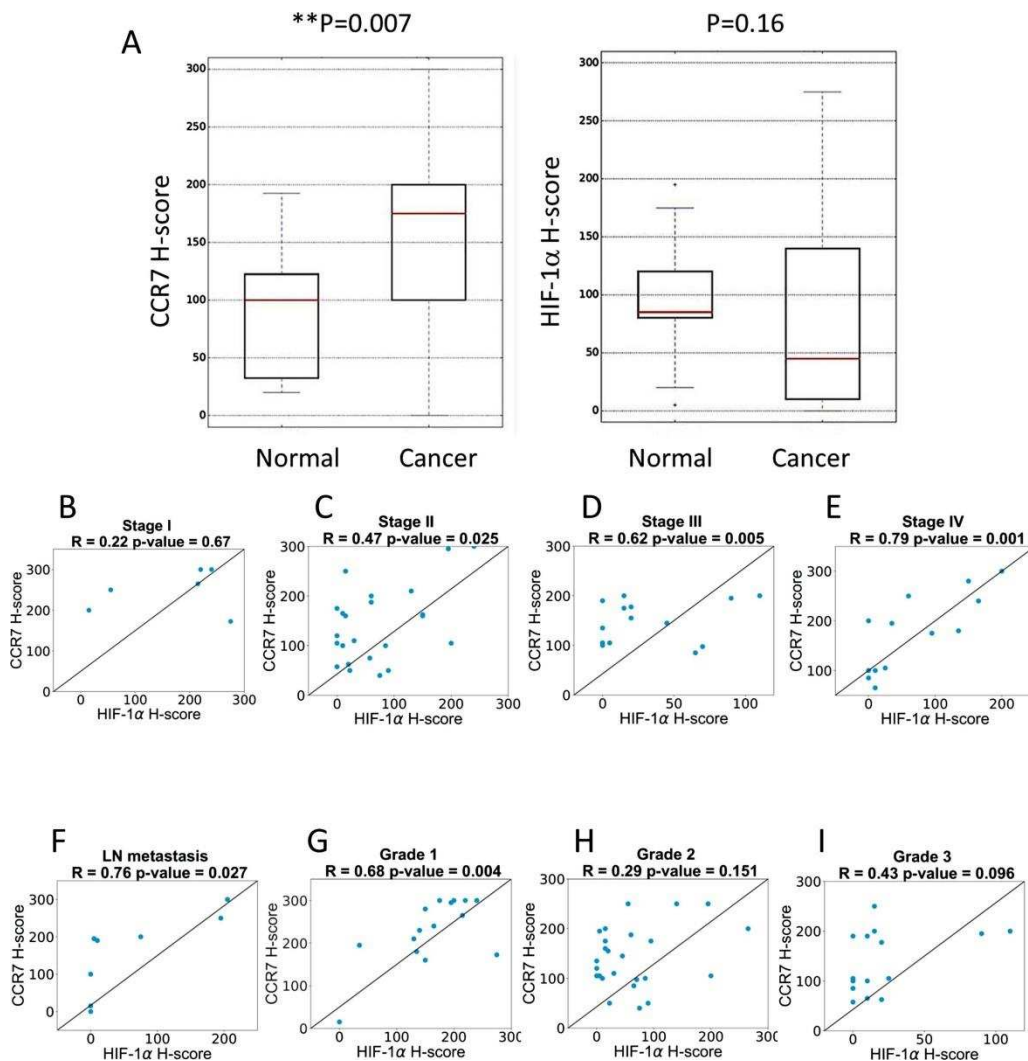


Figure 6. (A) Comparison of the range of H-score for CCR7 and HIF-1 α between non-malignant and malignant tissue samples show that CCR7 expression is elevated in malignant compared to non-malignant tissue (red line represent median value of H-scores in each case). (B-E) Analysis of the relative expression of CCR7 and HIF-1 α in each individual sample shows a correlation between the two for each clinical stage as well as for lymph node metastases (F-I). Analysis of the relative expression of CCR7 and HIF-1 α in each individual sample showed a correlation between the two in individual samples for all grades; with the highest correlation observed in grade 1.

An analysis of the relative expression of CCR7 and HIF-1 α in each individual tissue sample revealed a correlation (R) between the two for each clinical stage (Figure 6B-E), as well as for lymph node metastases (Figure 6F). Similarly, we observed a correlation between the relative expression of CCR7 and HIF-1 α in individual samples for all grades; with the highest correlation observed in grade 1 (R=0.68, P=0.004) (Figure 6G-I) suggesting that the level of differentiation of tumours may be relevant for the relationship between CCR7 and HIF-1 α .

Our findings are concordant with two previous studies in breast [35] and lung [36] cancer which also reported a correlation between the CCR7 and HIF-1 α expression, and studies

which associate another important chemokine receptor, CXCR4, to hypoxia and HIF-1 α [31, 32]. They support the hypothesis that hypoxia, particularly in the early stages of tumour development, may be involved in promoting the invasion and migration of head and neck cancer cells through CCR7 axis.

Grade	CCR7			HIF-1 α		
	Low (n)	High (n)	P	Low (n)	High (n)	P
non-malignant	9	2		9	2	
Grade 1	1	15	P=0.0001**	5	11	P=0.018*
Grade 2	11	15	P=0.26	23	3	P=0.6
Grade 3	9	7	P=0.23	16	0	P=0.16

Table 2: Association of high expression of CCR7 or HIF-1 α with head and neck cancer in different histological grades of the disease.

Conclusions

We have shown that in 2D monolayers, 3D multicellular spheroids, xenotransplanted cells and clinical tissue, there is a positive correlation between hypoxia and CCR7 expression. In clinical samples in particular, the correlation between hypoxia and CCR7 in the all clinical stages suggests the two are related.

Hypoxia is a key feature of head and neck tumours, is widely observed in the clinical setting, and is associated with resistance to radiotherapy, reduced therapeutic response, and a poorer clinical outcome. [53,54] The role of hypoxia in head and neck tumours is undoubtedly complex and acts through multiple pathways. However, understanding the mechanisms by which hypoxia can promote the tumour progression, provides opportunities to combat its negative impact on the disease. [55-59] Our results strongly associate hypoxia with the emergence of the expression of CCR7, complementing earlier observations by Ferris who has shown that release of CCL21 and CCL19 into the tumour microenvironment by invading lymphocytes can increase CCR7 expression through an autocrine loop. [10] Taken together, both results confirm a central role for the CCR7 axis in head and neck

tumours. In addition, in view of CCR7 being a negative prognostic factor for lymph node (LN) metastasis, [19-21] our findings suggests that hypoxia is likely to contribute to the development of a metastatic phenotype in head and neck cancers through upregulation of CCR7 signalling. Therefore, inhibition of CCR7 signalling by small molecule CCR7 antagonists [60] may prove to be a very useful adjunct therapy to be used in combination with existing treatments for head and neck cancers.

Acknowledgement

We wish to thank Al-Zarqa University for studentship to HAB.

Author contribution

Experimental work was carried out by HAB. Statistical analysis was carried out by EP. Xenografts were prepared by PAC and SDS. Scoring of the clinical tissue was carried out independently by LM and KDH. VV and KA designed experiments. Manuscript was written by KA and all authors reviewed the manuscript.

Competing financial interest statement

Authors declare no competing financial interests.

References

1. Hussein AA, Helder MN, de Visscher JG, Leemans CR, Braakhuis BJ, de Vet HCW, Forouzanfar T. (2017) Global incidence of oral and oropharynx cancer in patients younger than 45 years versus older patients: A systematic review. *Eur. J. Cancer* 82:115-127.
2. Ridge JA, Mehra R, Lango MN, Galloway, T (2016) <http://www.cancernetwork.com/cancer-management/head-and-neck-tumors> (accessed 27 July 2017)
3. N Kulbe H, Levinson NR, Balkwill F, Wilson JL. (2004) The chemokine network in cancer--much more than directing cell movement. *Int. J. Dev. Biol.* 48(5-6):489-96.
4. akata B, Fukunaga S, Noda E, Amano R, Yamada N, Hirakawa K (2008) Chemokine receptor CCR7 expression correlates with lymph node metastasis in pancreatic cancer. *Oncology* 74(1-2): 69-75.
5. Gunther K, Leier J, Henning G, Dimmler A, Weissbach R, Hohenberger W, Forster R (2005) Prediction of lymph node metastasis in colorectal carcinoma by expression of chemokine receptor CCR7. *Int. J. Cancer* 116 (5): 726-733. 10.1002/ijc.21123.

6. Mashino K, Sadanaga N, Yamaguchi H, Tanaka F, Ohta M, Shibuta K, Inoue H, Mori M (2002) Expression of chemokine receptor CCR7 is associated with lymph node metastasis of gastric carcinoma. *Cancer Res.*, 62(10): 2937-2941.
7. Shields JD, Emmett MS, Dunn DB, Joory KD, Sage LM, Rigby H, Mortimer PS, Orlando A, Levick JR, Bates DO (2007) Chemokine-mediated migration of melanoma cells towards lymphatics--a mechanism contributing to metastasis. *Oncogene* 26(21): 2997-3005.
8. Liu Y, Ji R, Li J, Gu Q, Zhao X, Sun T, Wang J, Li J, Du Q, Sun B (2010) Correlation effect of EGFR and CXCR4 and CCR7 chemokine receptors in predicting breast cancer metastasis and prognosis. *J. Exp. Clin. Cancer Res.* 29: 16.
9. Cabioglu N, Yazici MS, Arun B, Broglio KR, Hortobagyi GN, Price JE, Sahin A (2005) CCR7 and CXCR4 as novel biomarkers predicting axillary lymph node metastasis in T1 breast cancer. *Clin Cancer Res.* 11(16): 5686-5693.
10. Mburu YK, Wang J, Wood MA, Walker WH, Ferris RL (2006) CCR7 mediates inflammation-associated tumor progression. *Immunol Res.* 36(1-3):61-72.
11. da Silva JM, Soave DF, Moreira Dos Santos TP, Batista AC, Russo RC, Teixeira MM, da Silva TA (2016) Significance of chemokine and chemokine receptors in head and neck squamous cell carcinoma: A critical review. *Oral Oncol.* 56: 8-16.
12. Sancho M, Vieira JM, Casalou C, Mesquita M, Pereira T, Cavaco BM, Dias S, Leite V (2006) Expression and function of the chemokine receptor CCR7 in thyroid carcinomas. *J. Endocrinology* 191(1):229-238.
13. Wang J, Xi L, Hunt JL, Gooding W, Whiteside TL, Chen Z, Godfrey TE, Ferris RL (2004) Expression pattern of chemokine receptor 6 (CCR6) and CCR7 in squamous cell carcinoma of the head and neck identifies a novel metastatic phenotype. *Cancer Res.* 64(5):1861-1866.
14. Ishida K, Iwahashi M, Nakamori M, Nakamura M, Yokoyama S, Iida T, Naka T, Nakamura Y, Yamaue H. (2009) High CCR7 mRNA expression of cancer cells is associated with lymph node involvement in patients with esophageal squamous cell carcinoma. *Int. J. Oncol.* 34(4): 915-922
15. T. Irino, H. Takeuchi, S. Matsuda, Y. Saikawa, H. Kawakubo, N. Wada, Takahashi T, Nakamura R, Fukuda K, Omori T, Kitagawa Y (2014) CC-Chemokine receptor CCR7: a key molecule for lymph node metastasis in esophageal squamous cell carcinoma *BMC Cancer* 14: 291
16. Shang ZJ, Liu K, Shao Z (2009) Expression of chemokine receptor CCR7 is associated with cervical lymph node metastasis of oral squamous cell carcinoma. *Oral Oncol.* 45:480-485
17. Xia X, Liu K, Zhang H, Shang Z. (2015) Correlation between CCR7 expression and LN metastasis of human tongue carcinoma. *Oral Dis.* 21(1):123-131.

18. Oliveira-Neto HH, de Souza PPC, da Silva MRB, Mendonca EF, Silva TA, Batista AC (2013) The expression of chemokines CCL19, CCL21 and their receptor CCR7 in oral squamous cell carcinoma and its relevance to cervical lymph node metastasis. *Tumor Biol.* 34(1): 65-70.
19. Pitkin L, Luangdilok S, Corbishley C, Wilson POG, Dalton P, Bray D, Mady S, Williamson P, Odutoye T, Evans PR, Syrigos KN, Nutting CM, Barbachano Y, Eccles S, Harrington KJ (2007) Expression of CC chemokine receptor 7 in tonsillar cancer predicts cervical nodal metastasis, systemic relapse and survival. *Br. J. Cancer* 97(5): 670-677
20. Tsuzuki H, Takahashi N, Kojima A, Narita N, Sunaga H, Takabayashi T, Shigeharu F (2006) Oral and oropharyngeal squamous cell carcinomas expressing CCR7 have poor prognoses. *Auris Nasus Larynx*, 33: 37-42.
21. Liu XY, Song L, Wang Z (2013) CCR7: A Metastasis and Prognosis Indicator of Postoperative Patients with Esophageal Carcinoma. *Hepato-gastroenterology* 60(124): 747-750
22. Wang J, Zhang X, Thomas SM, Grandis JR, Wells A, Chen Z, Ferris RL (2005) Chemokine receptor 7 activates phosphoinositide-3 kinase-mediated invasive and prosurvival pathways in head and neck cancer cells independent of EGFR. *Oncogene* 24(38): 5897-5904
23. Liu FY, Safdar J, Li ZN, Fang QG, Zhang X, Xu ZF, Sun C (2014) CCR7 Regulates Cell Migration and Invasion through JAK2/STAT3 in Metastatic Squamous Cell Carcinoma of the Head and Neck. *BioMed Res. Int.* Article Number: 415375
24. Guo N, Liu FY, Yang LL, Huang JY, Ding X, Sun CF (2014) Chemokine receptor 7 enhances cell chemotaxis and migration of metastatic squamous cell carcinoma of head and neck through activation of matrix metalloproteinase-9. *Oncol. Rep.* 32(2): 794-800.
25. Liu FY, Safdar J, Li ZN, Fang QG, Zhang X, Xu ZF, Sun CF (2014) CCR7 regulates cell migration and invasion through MAPKs in metastatic squamous cell carcinoma of head and neck. *Int. J. Oncol.* 45(6): 2502-2510.
26. Li P, Liu FY, Sun LY, Zhao ZJ, Ding X, Shang DH, Xu ZF, Sun CF (2011) Chemokine receptor 7 promotes cell migration and adhesion in metastatic squamous cell carcinoma of the head and neck by activating integrin alpha v beta 3 *Int. J. Mol. Med.* 27(5): 679-687
27. McKeown SR (2014) Defining normoxia, physoxia and hypoxia in tumours-implications for treatment response. *Br. J. Radiol.* 87(1035):20130676.
28. Lu X, Kang YB. (2010) Hypoxia and Hypoxia-Inducible Factors: Master Regulators of Metastasis. *Clin. Cancer Res.* 16(24): 5928-5935.
29. Fang H, DeClerck YA, (2013) Targeting the Tumor Microenvironment: From Understanding Pathways to Effective Clinical Trials. *Cancer Res.* 73(16): 4965-4977

30. Curry JM, Sprandio J, Cognetti D, Luginbuhl A, Bar-ad V, Pribitkin E, Tuluc M (2014) Tumor Microenvironment in Head and Neck Squamous Cell Carcinoma. *Semin. Oncol.* 41(2): 217-234
31. Swartz JE, Pothan AJ, Stegeman I, Willems SM, Grolman W. (2015) Clinical implications of hypoxia biomarker expression in head and neck squamous cell carcinoma: a systematic review. *Cancer Med.* 4(7):1101-1116.
32. Cronin PA, Wang JH, Redmond HP (2010) Hypoxia increases the metastatic ability of breast cancer cells via upregulation of CXCR4. *BMC Cancer* 10: 225.
33. Ishikawa T, Nakashiro K, Klosek SK, Goda H, Hara S, Uchida D, Hamakawa H,. (2009) Hypoxia enhances CXCR4 expression by activating HIF-1 in oral squamous cell carcinoma. *Oncol. Rep.* 21(3): 707-712.
34. Lin SS, Wan SY, Sun L, Hu JL, Fang DD, Zhao RP, Yuan ST, Zhang LY (2012) Chemokine C-C motif receptor 5 and C-C motif ligand 5 promote cancer cell migration under hypoxia *Cancer Sci.* 103(5): 904-912.
35. Wilson JL, Burchell J, Grimshaw MJ (2006) Endothelins induce CCR7 expression by breast tumor cells via endothelin receptor A and hypoxia-inducible factor-1. *Cancer Res.* 66(24): 11802-11807.
36. Li Y, Qiu XS, Zhang SY, Zhang QF, Wang EH (2009) Hypoxia induced CCR7 expression via HIF-1 alpha and HIF-2 alpha correlates with migration and invasion in lung cancer cells. *Cancer Biol Ther.* 8(4): 322-330.
37. Schindelin J, Arganda-Carreras I, Frise E, Kaynig V, Longair M, Pietzsch T, Preibisch S, Rueden C, Saalfeld S, Schmid B, Tinevez JY, White DJ, Hartenstein V, Eliceiri K, Tomancak P, Cardona A Fijj: an open-source platform for biological-image analysis. *Nat. Methods* 9(7): 676–682.
38. Hirsch FR, Varella-Garcia M, Bunn PA Jr, Di Maria MV, Veve R, Bremmes RM, Barón AE, Zeng C, Franklin WA (2003) Epidermal growth factor receptor in non-small-cell lung carcinomas: Correlation between gene copy number and protein expression and impact on prognosis. *J. Clin. Oncol.* 21:3798-3807.
39. Na IK, Busse A, Scheibenbogen C, Ghadjar P, Coupland SE, Letsch A, Loddenkemper C, Stroux A, Bauer S, Thiel E, Keilholz U (2008) Identification of truncated chemokine receptor 7 in human colorectal cancer unable to localize to the cell surface and unreactive to external ligands. *Int. J. Cancer* 123: 1565-1572.
40. Haessler U, Pisano M, Wu M, Swartz MA. (2011) Dendritic cell chemotaxis in 3D under defined chemokine gradients reveals differential response to ligands CCL21 and CCL19. *Proc. Natl. Acad. Sci. U. S. A.*;108(14):5614-9.
41. Raju R, Gadakh S, Gopal P, George B, Advani J, Soman S, Prasad TS, Girijadevi R. (2015) Differential ligand-signaling network of CCL19/CCL21-CCR7 system. *Database pii: bav106.*

42. Lee JM, Mhaweche-Fauceglia P, Lee N, Parsanian LC, Lin YG, Gayther SA, Lawrenson K. (2013) A three-dimensional microenvironment alters protein expression and chemosensitivity of epithelial ovarian cancer cells in vitro. *Lab Invest.* 93(5):528-42.
43. Eckert AW, Wickenhauser C, Salins PC, Kappler M, Bukur J, Seliger B. (2016) Clinical relevance of the tumor microenvironment and immune escape of oral squamous cell carcinoma. *J. Transl. Med.* 14:85.
44. Elkashef SM, Allison SJ, Sadiq M, Basheer HA, Ribeiro Morais G, Loadman PM, Pors K, Falconer RA (2016) Polysialic acid sustains cancer cell survival and migratory capacity in a hypoxic environment. *Sci. Reports*, 6, 33026.
45. Semenza GL. (2013) HIF-1 mediates metabolic responses to intratumoral hypoxia and oncogenic mutations. *J. Clin. Invest.* 123: 3664-3671.
46. Vaupel P, Mayer A. (2007) Hypoxia in cancer: significance and impact on clinical outcome. *Cancer Metastasis Rev.* 26(2): 225-239.
47. Déry MA, Michaud MD, Richard DE (2005) Hypoxia-inducible factor 1: regulation by hypoxic and non-hypoxic activators. *Int. J. Biochem. Cell Biol.* 37(3):535-40.
48. Agani F, Jiang BH (2013) Oxygen-independent regulation of HIF-1: novel involvement of PI3K/AKT/mTOR pathway in cancer. *Curr. Cancer Drug Targets* 13(3):245-51.
49. Yuan Y, Hilliard G, Ferguson T, Millhorn DE (2003) Cobalt inhibits the interaction between hypoxia-inducible factor-alpha and von Hippel-Lindau protein by direct binding to hypoxia-inducible factor-alpha. *J Biol. Chem.* 278(18):15911-15916.
50. Hirschhaeuser F, Menne H, Dittfeld C, West J, Mueller-Klieser W, Kunz-Schughart, LA (2010) Multicellular tumor spheroids: an underestimated tool is catching up again. *J. Biotechnol.* 148: 3-15.
51. Varia MA, Calkins-Adams DP, Rinker LH, Kennedy AS, Novotny DB, Fowler WC Jr, Raleigh JA. (1998) Pimonidazole: a novel hypoxia marker for complementary study of tumor hypoxia and cell proliferation in cervical carcinoma. *Gynecol Oncol.* 71(2):270-277.
52. Scholzen T, Gerdes J. (2000) The Ki-67 protein: from the known and the unknown. *J. Cell Physiol.* 182(3):311-322.
53. Bredell MG, Ernst J, El-Kochairi I, Dahlem Y, Ikenberg K, Schumann DM (2016) Current relevance of hypoxia in head and neck cancer. *Oncotarget* 7(31): 50781-50804.
54. Janssen HL, Haustermans KM, Balm AJ, Begg AC (2005) Hypoxia in head and neck cancer: how much, how important? *Head Neck* 27(7): 622-638.
55. Overgaard J (2011) Hypoxic modification of radiotherapy in squamous cell carcinoma of the head and neck - A systematic review and meta-analysis. *Radiother Oncol* 100(1): 22-32.

56. Hsu HW, Wall NR, Hsueh CT, Kim S, Ferris RL, Chen CS, Mirshahidi S (2014) Combination antiangiogenic therapy and radiation in head and neck cancers. *Oral Oncol.* 50(1): 19-26.
57. Horsman MR, Overgaard J. (2016) The impact of hypoxia and its modification of the outcome of radiotherapy. *J. Radiat. Res.* 57 Suppl 1:i90-i98.
58. Baumann R, Depping R, Delaperriere M, Dunst J (2016) Targeting hypoxia to overcome radiation resistance in head & neck cancers: real challenge or clinical fairytale? *Expert Rev. Anticancer Ther.* 16(7): 751-758.
59. Gammon L, Mackenzie IC (2016) Roles of hypoxia, stem cells and epithelial-mesenchymal transition in the spread and treatment resistance of head and neck cancer. *J. Oral Pathol. Med.* 45(2): 77-82.
60. Ahmed M, Basheer HA, Ayuso JM, Ahmet D, Mazzini M, Patel R, Shnyder SD, Vinader V, Afarinkia K. (2017) Agarose Spot as a Comparative Method for in situ Analysis of Simultaneous Chemotactic Responses to Multiple Chemokines. *Sci. Reports*, 7, Article number: 1075.

Supplementary information

Supplementary Information S1: Characteristics of microarrays clinical sample

position	gender	age	organ	pathology	grade	stage	TNM	type
A1	F	61	Oral cavity	Squamous cell carcinoma of palate	1	I	T1N0M0	Malignant
A2	M	61	Lip	Squamous cell carcinoma of lower lip	1	I	T1N0M0	Malignant
A3	M	77	Lip	Squamous cell carcinoma of lower lip	1	I	T1N0M0	Malignant
A4	F	75	Oral cavity	Squamous cell carcinoma of upper jaw	1	I	T1N0M0	Malignant
A5	M	67	Oral cavity	Squamous cell carcinoma of right palate	1	II	T2N0M0	Malignant
A6	M	50	Tongue	Squamous cell carcinoma of root of tongue	1	III	T3N1M0	Malignant
A7	M	66	Pharynx	Squamous cell carcinoma of pharynx	1	IVA	T3N2M0	Malignant
A8	M	49	Gingiva	Squamous cell carcinoma of right gingiva	1	IVA	T4N0M0	Malignant
A9	M	55	Pharynx	Squamous cell carcinoma of epiglottis	1	IVA	T4N0M0	Malignant
A10	M	57	Pharynx	Squamous cell carcinoma of oropharynx	1	IV	T4N0M0	Malignant
B1	M	74	Nose	Squamous cell carcinoma of root of nose	2	II	T2N0M0	Malignant
B2	M	90	Cheek	Squamous cell carcinoma of cheek	-	II	T2N0M0	Malignant
B3	M	72	Larynx	Squamous cell carcinoma of larynx	1	II	T2N0M0	Malignant
B4	F	61	Oral cavity	Squamous cell carcinoma of right mandible	1	II	T2N0M0	Malignant
B5	M	50	Larynx	Squamous cell carcinoma of larynx	1	III	T2N1M0	Malignant
B6	M	67	Larynx	Squamous cell carcinoma of larynx	2	III	T3N1M0	Malignant
B7	M	58	Larynx	Squamous cell carcinoma of larynx	2	III	T3N1M1	Malignant
B8	M	52	Nose	Squamous cell carcinoma of nasopharynx	2	I	T1N0M0	Malignant
B9	M	60	Tongue	Squamous cell carcinoma of tongue	2	II	T2N0M0	Malignant
B10	M	60	Tongue	Squamous cell carcinoma of tongue	2	II	T2N0M0	Malignant
C1	M	67	Larynx	Squamous cell carcinoma of throat	3	II	T2N0M0	Malignant
C2	M	48	Cheek	Squamous cell carcinoma of cheek	1	II	T2N0M0	Malignant
C3	M	70	Oral cavity	Squamous cell carcinoma of right mandible	2	II	T2N0M0	Malignant
C4	M	43	Oral cavity	Squamous cell carcinoma of right mandible	2	II	T2N0M0	Malignant
C5	M	56	Pharynx	Squamous cell carcinoma of pharynx	2	II	T2N0M0	Malignant
C6	M	45	Cheek	Squamous cell carcinoma of right cheek	-	II	T2N0M0	Malignant
C7	M	47	Larynx	Squamous cell carcinoma of larynx	2	II	T2N0M0	Malignant
C8	M	61	Pharynx	Squamous cell carcinoma of epiglottis	-	II	T2N0M0	Malignant
C9	M	50	Larynx	Squamous cell carcinoma of larynx	2	II	T2N0M0	Malignant
C10	F	38	Lip	Squamous cell carcinoma of lower lip	2	II	T2N0M0	Malignant
D1	M	47	Larynx	Squamous cell carcinoma of larynx	3	III	T2N1M0	Malignant
D2	F	50	Pharynx	Squamous cell carcinoma of hypopharynx	2	III	T2N1M0	Malignant
D3	M	71	Pharynx	Squamous cell carcinoma of hypopharynx	2	III	T2N1M0	Malignant
D4	M	44	Pharynx	Squamous cell carcinoma of hypopharynx	2	III	T2N1M0	Malignant
D5	M	61	Pharynx	Squamous cell carcinoma of epiglottis	2	III	T2N1M0	Malignant
D6	M	54	Oral cavity	Squamous cell carcinoma of left upper jaw	2	III	T3N0M0	Malignant
D7	M	61	Pharynx	Squamous cell carcinoma of hypopharynx	3	III	T3N0M0	Malignant
D8	M	58	Larynx	Squamous cell carcinoma of larynx	3	III	T3N0M0	Malignant

D9	M	63	Pharynx	Squamous cell carcinoma of epiglottis	2	III	T3N1M0	Malignant
D10	M	71	Pharynx	Squamous cell carcinoma of epiglottis	3	III	T3N1M0	Malignant
E1	M	51	Pharynx	Squamous cell carcinoma of left pharynx	2	III	T3N1M0	Malignant
E2	M	55	Larynx	Squamous cell carcinoma of larynx	2	III	T3N1M0	Malignant
E3	M	75	Oral cavity	Squamous cell carcinoma of maxillary sinus	2	IV	T4N0M0	Malignant
E4	M	56	Pharynx	Squamous cell carcinoma of epiglottis	1	IVA	T4N0M0	Malignant
E5	M	57	Larynx	Squamous cell carcinoma of larynx	-	IVA	T4N0M0	Malignant
E6	M	49	Larynx	Squamous cell carcinoma of larynx	3	IVA	T4N1M0	Malignant
E7	F	69	Cheek	Squamous cell carcinoma of right cheek	2	I	T2N0M0	Malignant
E8	M	29	Larynx	Squamous cell carcinoma of larynx	-	II	T2N0M0	Malignant
E9	F	56	Lip	Squamous cell carcinoma of oral lip	2	II	T2N0M0	Malignant
E10	M	50	Oral cavity	Squamous cell carcinoma of maxillary sinus	2	II	T2N0M0	Malignant
F1	M	50	Tongue	Squamous cell carcinoma of tongue	3	II	T2N0M0	Malignant
F2	M	64	Larynx	Squamous cell carcinoma of larynx	3	II	T2N0M0	Malignant
F3	M	49	Larynx	Squamous cell carcinoma of larynx	3	III	T2N1M0	Malignant
F4	F	42	Nose	Squamous cell carcinoma of nasal sinus	3	III	T3N0M0	Malignant
F5	M	50	Larynx	Squamous cell carcinoma of larynx	3	III	T3N1M0	Malignant
F6	M	58	Larynx	Squamous cell carcinoma of larynx	3	IV	T2N2N0	Malignant
F7	M	75	Nose	Squamous cell carcinoma of nasal sinus	3	IV	T4N0M0	Malignant
F8	M	48	Pharynx	Squamous cell carcinoma of hypopharynx	3	IV	T4N0M0	Malignant
F9	M	74	Pharynx	Squamous cell carcinoma of hypopharynx	-	IV	T4N0M0	Malignant
F10	M	65	Larynx	Squamous cell carcinoma of larynx	3	IV	T3N2M0	Malignant
G1	F	32	Oral cavity	Carcinoma sarcomatodes of maxillary sinus	-	II	T2N0M0	Malignant
G2	F	40	Lymph node	Metastatic mucoepidermoid carcinoma	-	-	-	Metastasis
G3	M	67	Lymph node	Metastatic mucoepidermoid carcinoma	-	-	-	Metastasis
G4	M	45	Lymph node	Metastatic mucoepidermoid carcinoma	-	-	-	Metastasis
G5	M	47	Lymph node	Metastatic squamous cell carcinoma	1	-	-	Metastasis
G6	M	48	Lymph node	Metastatic squamous cell carcinoma	2	-	-	Metastasis
G7	M	53	Lymph node	Metastatic squamous cell carcinoma	3	-	-	Metastasis
G8	F	45	Lymph node	Metastatic squamous cell carcinoma	2	-	-	Metastasis
G9	F	52	Lymph node	Metastatic acinic cell carcinoma	-	-	-	Metastasis
G10	M	38	Tongue	Adjacent normal tongue tissue	-	-	-	NAT
H1	M	28	Tongue	Tongue tissue	-	-	-	Normal
H2	F	27	Tongue	Tongue tissue	-	-	-	Normal
H3	M	48	Tongue	Tongue tissue	-	-	-	Normal
H4	F	42	Tongue	Adjacent normal tongue tissue	-	-	-	NAT
H5	F	15	Tongue	Tongue tissue	-	-	-	Normal
H6	F	19	Tongue	Tongue tissue	-	-	-	Normal
H7	M	35	Tongue	Tongue tissue	-	-	-	Normal
H8	F	18	Tongue	Tongue tissue	-	-	-	Normal
H9	F	19	Tongue	Tongue tissue	-	-	-	Normal
H10	M	28	Tongue	Tongue tissue	-	-	-	Normal

Supplementary Information S2: Representative images from immunohistochemical staining of the tumour microarray for expression level of CCR7 (**A-D**) and HIF-1 α (**E-H**) in head and neck tumours. (**A** and **E**) strong staining; (**B** and **F**) medium staining; (**C** and **G**) weak staining; (**D** and **H**) control.

